

# Dual-modal Dynamic Traceback Learning for Medical Report Generation

Shuchang Ye, Mingyuan Meng, Mingjian Li and Dagan Feng and Jinman Kim

The University of Sydney

{shuchang.ye, dagan.feng, jinman.kim}@sydney.edu.au, {mmen2292, mili3287}@uni.sydney.edu.au

## Abstract

With increasing reliance on medical imaging in clinical practices, automated report generation from medical images is in great demand. Existing report generation methods typically adopt an encoder-decoder deep learning framework to build a uni-directional image-to-report mapping. However, such a framework ignores the bi-directional mutual associations between images and reports, thus incurring difficulties in associating the intrinsic medical meanings between them. Recent generative representation learning methods have demonstrated the benefits of dual-modal learning from both image and text modalities. However, these methods exhibit two major drawbacks for medical report generation: 1) they tend to capture morphological information and have difficulties in capturing subtle pathological semantic information, and 2) they predict masked text rely on both unmasked images and text, inevitably degrading performance when inference is based solely on images. In this study, we propose a new report generation framework with dual-modal dynamic traceback learning (DTrace) to overcome the two identified drawbacks and enable dual-modal learning for medical report generation. To achieve this, our DTrace introduces a traceback mechanism to control the semantic validity of generated content via self-assessment. Further, our DTrace introduces a dynamic learning strategy to adapt to various proportions of image and text input, enabling report generation without reliance on textual input during inference. Extensive experiments on two well-benchmarked datasets (IU-Xray and MIMIC-CXR) show that our DTrace outperforms state-of-the-art medical report generation methods.

## 1 Introduction

With an increasing reliance on medical images in clinical practices, there is a growing need for automated report generation from medical images [Messina *et al.*, 2022], which has the potential to streamline the manual diagnostic process by reducing the repetitive workload of clinical experts. However,

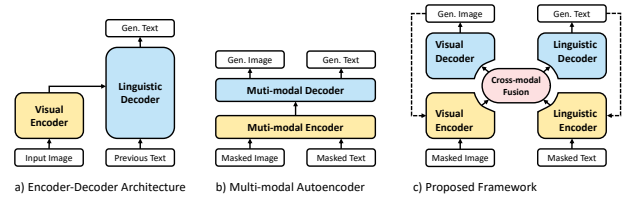


Figure 1: Illustration of different generative frameworks. (a) Common uni-modal encoder-decoder framework, (b) Dual-modal masked encoder-decoder framework for generative representation learning (GRL), and (c) Our proposed framework with dual-modal dynamic traceback learning (DTrace).

medical report generation, despite advances in deep learning, is problematic due to the complexity of associating the intrinsic medical meanings between the corresponding reports and images. This is because medical images often exhibit subtle regions representing critical diagnostic meanings, such as a tumor region, and medical reports also rely on a small subset of keywords to represent diagnosis-relevant information. Hence, it is crucial to develop a method that can capture and associate this nuanced information to preserve the intrinsic medical meanings within medical images and reports.

Existing medical report generation methods usually rely on an encoder-decoder framework (Figure 1a) that performs uni-modal learning to build a uni-directional mapping from images to reports [Vaswani *et al.*, 2017; Chen *et al.*, 2020; Wang *et al.*, 2022b; You *et al.*, 2021]. However, such a framework is limited in associating intrinsic medical meanings as it ignores the bi-directional mutual associations between images and reports. Modeling of multi-modal information to build mutual associations is common in neural learning systems, and it has been demonstrated to facilitate understanding of cross-modal knowledge [Lu *et al.*, 2022]. Recently, Generative Representation Learning (GRL) methods have exploited dual-modal learning and generation [Devlin *et al.*, 2018; He *et al.*, 2022; Geng *et al.*, 2022], where image and report reconstruction are jointly performed in a dual-modal masked encoder-decoder framework (Figure 1b). These methods aim to learn the latent space representations by masking inputs and subsequently reconstructing the original inputs based on the unmasked information. Although these methods have brought significant advancements in dual-modal learning,

they exhibit considerable gaps when adopted for medical report generation due to two primary drawbacks:

First, GRL methods prioritize capturing morphological information (e.g., organ shape and report structure) and have difficulties in capturing subtle pathological semantic information (e.g., lesion location and spread of disease). For image reconstruction, GRL methods usually learn to minimize pixel-level discrepancies between the original and reconstructed images. However, this learning approach inadvertently leads to an over-simplified pixel-matching task that ignores image semantic information with pathological context. For report reconstruction, GRL methods usually tend to predict frequently observed words to achieve a high overlap rate between the original and reconstructed reports. Due to the word imbalance in medical reports, where keywords signifying pathology appear infrequently, this learning approach potentially leads to the generation of clinically-flawed templated reports. Further, there exists inherent variability in the report descriptions for the same medical images, such as the order of reporting (e.g., starting from the disease sites or from image acquisition protocol) and the lexical choices employed to convey the severity of symptoms. However, the loss functions of GRL methods typically operate at the word level, which cannot measure the quality of generated reports from the sentence level with semantic contextual information.

Second, GRL methods focus on predicting masked images and text from their unmasked counterparts, which usually require a large amount of unmasked information to achieve text reconstruction [Devlin *et al.*, 2018; Geng *et al.*, 2022], with the mask ratio for the text being limited to a low range,  $\approx 15\%$  (most textual information retained as the input). In contrast, in medical report generation, inference is based solely on images. Such a shift can lead to a performance decline in report generation, as GRL methods are not designed to handle inference from images alone without accompanying text.

In this study, we propose a novel report generation framework with dual-modal dynamic traceback learning (DTrace), which overcomes the drawbacks of GRL methods and introduces dual-modal learning for medical report generation. To this end, our DTrace introduces the following contributions:

- Our DTrace performs dual-modal learning for medical report generation (Figure 1c), where the intrinsic medical associations between images and reports are explored through joint learning of bi-directional image-to-report and report-to-image generation.
- We propose a traceback mechanism in the DTrace to control the semantic validity of the generated content via its inherent feature extraction capability. This process involves the reintegration of the generated images and textual reports into their respective encoders, facilitating a mechanism of self-assessment.
- We propose a dynamic learning strategy in the DTrace to accommodate inputs of any image-text proportions. This enables our DTrace to effectively learn from both modalities during training, while still relying solely on image information during inference. The loss weights corresponding to the image and report generation are

also dynamically adjusted, allowing the model to be effectively trained with varying input proportions.

Extensive experiments on two well-benchmarked datasets (IU-Xray and MIMIC-CXR) show that our DTrace outperforms state-of-the-art medical report generation methods.

## 2 Related Work

### 2.1 Medical Report Generation

Traditional medical report generation methods rely on rule- or template-based methods [Cawsey *et al.*, 1997]. Rule-based methods often fall short in handling different scenarios and capturing language subtleties, while template-based methods are dependent on template quality and adaptability. With the paradigm shift in Computer Vision (CV) and Natural Language Processing (NLP), deep learning-based medical report generation methods have achieved promising performance and attained wide attention [Messina *et al.*, 2022].

Deep learning-based report generation can be traced back to the invention of encoder-decoder architecture. Within this framework, images were transmuted into representative vectors encapsulating salient information through a visual encoder, followed by a linguistic decoder to predict text [Vinyals *et al.*, 2015]. Subsequent studies primarily focused on enhancing the capabilities of the visual encoder and the linguistic decoder [Stefanini *et al.*, 2021], e.g., from Convolutional Neural Networks (CNN) and Recurrent Neural Networks (RNN) to Vision Transformer (ViT) and Transformer [Wang *et al.*, 2022b]. Recently, the interaction and communication between the visual encoder and linguistic decoder have also attracted wide attention. For example, R2GenCMN [Chen *et al.*, 2021] proposed to unify the visual and linguistic representations by sharing a vector pool across the visual encoder and linguistic decoder. XProNet [Wang *et al.*, 2022a] further improved the R2GenCMN by monitoring the vector pool with pathological labels. These methods improved cross-modal communication and achieved state-of-the-art medical report generation performance. However, they still relied on a uni-directional image-to-report mapping and ignored the bi-directional mutual image-report associations. Based on our review, our DTrace is the first report generation framework that incorporates dual-modal learning and generation.

### 2.2 Generative Representation Learning

GRL methods learn the latent space representations by training the model to reconstruct the masked inputs based on the unmasked information. Masked Image Modeling (MAE) [He *et al.*, 2022] and Masked Language Modeling (BERT) [Devlin *et al.*, 2018] are prevalent pre-training techniques in CV and NLP. BERT learned the word latent representations by training the model to predict the masked content based on the surrounding words. Then, MAE employed a similar strategy in images, where the images were split into patches and the model was trained to reconstruct the randomly masked patches. Recently, M3AE [Geng *et al.*, 2022] exploited dual-modal learning and generation, where image and text reconstruction were jointly performed with a dual-modal masked encoder-decoder framework to enhance the comprehension of

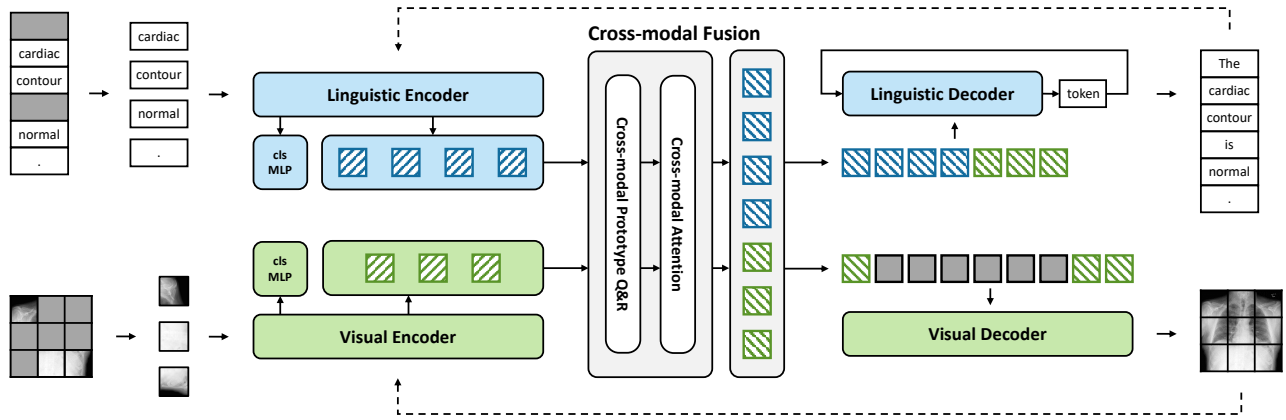


Figure 2: Our DTrace with dual-modal dynamic traceback learning. Solid and dashed lines indicate forward and traceback stages.

cross-modal associations. These GRL methods were widely adopted as a pre-training step to enhance the performance of downstream tasks, such as disease classification [Xiao *et al.*, 2023] and medical visual question answering [Liu *et al.*, 2023].

The capability of reconstructing masked text provides the potential for report generation. However, GRL methods were seldom applied to medical report generation due to the two drawbacks that we identified above. Recently, MedViLL [Moon *et al.*, 2022] applied GRL framework to medical report generation (as one of the downstream tasks) by progressively replacing mask tokens with predicted language tokens. Unfortunately, its performance was limited (0.066 in BLEU4 in the MIMIC-CXR dataset) as it was not trained to handle situations where text information is not available.

### 3 Method

#### 3.1 Network Architecture

The architecture of our DTrace is illustrated in Figure 2, comprising of five key components: a visual encoder, a visual decoder, a linguistic encoder, a linguistic decoder, and a cross-modal fusion module. The visual encoder processes partially masked images to extract incomplete pathological information. Simultaneously, fragmented textual information is also processed by the linguistic encoder to extract incomplete pathological information. Then, the extracted information is fed into the cross-modal fusion module, where a cross-attention mechanism is employed to foster the interaction between the visual and linguistic domains, thereby ameliorating the semantic deficits in both modalities. After this, the enriched information is conveyed to the visual and linguistic decoders correspondingly, so as to restore the masked images and reports to their original unmasked states. We will briefly introduce the five key components below and offer their detailed architectural settings in the supplementary materials.

##### Visual Encoder

Consistent with the common practice of MAE, medical images were split into patches and then were randomly masked. The visual encoder was a standard ViT [Dosovitskiy *et al.*,

2020], which mapped the unmasked patches into latent representations and then performed multi-label classification to predict the disease labels extracted via Chexpert [Irvin *et al.*, 2019].

##### Linguistic Encoder

Medical reports were mapped into embedded text tokens following the standard pre-processing steps [Devlin *et al.*, 2018]. Then, these tokens were randomly masked and fed into the linguistic encoder. The linguistic encoder was a classic text transformer block [Vaswani *et al.*, 2017].

##### Cross-Modal Fusion Module

The features extracted from both the encoders were projected to a pre-defined dimension, which then were then concatenated and fed to a cross-modal attention module [Geng *et al.*, 2022] for information interchange. The resultant features were subsequently separated and mapped into latent representations via Multi-layer Perceptrons (MLPs) [Taud and Mas, 2018].

##### Visual Decoder

The masked tokens were reinstated to their original positions, aligning with the unmasked encoding tokens. Following this, a lite version of ViT [He *et al.*, 2022] was used to restore the masked patches.

##### Linguistic Decoder

We adopted a relational memory Transformer [Chen *et al.*, 2020] to perform report generation. Taking previously generated text as the value, the decoder treated the concatenation of image patches and text patches as the query and key of the self-attention module to predict the next subsequent word.

#### 3.2 Traceback Mechanism

The traceback mechanism was designed to supervise the medical validity of generated items, which involves two stages: forward and traceback, as illustrated in Figure 3. The supervision is realized by augmenting the encoders' capacity to identify pathological information during the forward stage. Subsequently, during the traceback stage, these encoders guided the model in a self-assessment process, where the generated images and text reports were fed back to their

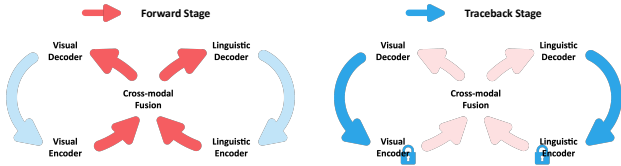


Figure 3: Dynamic traceback learning with forward stage (left) and traceback stage (right). The lock means that there is no gradient descent in back-propagation.

corresponding encoders. This self-assessment mechanism allowed the model to evaluate the semantic coherence and relevance of its outputs in relation to the training data and predefined criteria. As a result, the model can iteratively adjust and refine its generation process, enhancing the medical correctness and contextual appropriateness of the content it produces.

### Forward Stage

In the forward stage, our DTrace was trained to 1) detect diseases and 2) reconstruct images and generate reports. To achieve disease detection, we integrated a multi-label classification head to the encoders, minimizing the visual and linguistic binary cross-entropy loss between predicted probability distribution and disease labels extracted by Chexpert, named diagnostic loss,  $DLoss$ . For image reconstruction, pixel level mean-square-error (MSE) was minimized. For report generation, a cross-entropy (CE) loss of word prediction from the vocabulary is minimized.

### Traceback Stage

In the traceback stage, the reconstructed images and generated reports were redirected to their corresponding encoders to compute  $DLoss$ . To prevent potential performance decline in the encoders due to learning incorrect decision-making patterns, the gradient descent of the encoders was initially disabled. This aimed to refine the reconstructed images and generated reports to encapsulate the medical knowledge acquired by the encoders. As the performance of the encoders improved over time, the performance of the remaining components of the model was consequently propelled towards improved performance, creating a reinforcing cycle.

## 3.3 Dynamic Learning Strategy

Existing dual-modal GRL methods incurred performance degradation when generating reports from images alone. To address this limitation, the dynamic learning strategy was proposed to enhance the generalizability of the model to perform dual-modal generation given any percentage of text and image inputs. This was achieved through training with a range of complementary image and text mask ratios. This complementary relation aimed to guarantee sufficient shared information and to ensure that each modality can consistently derive some information from the other. It also incorporated a self-adjustment mechanism for loss weights, dynamically adapting to changes in the mask ratios. In the subsequent sections, the mathematical rationale behind the adjustment of loss weights during the forward and traceback stages was presented.

### Forward Stage

The loss weights assigned to generation tasks were proportional to their mask rates, facilitating more effective cross-modal communication. Meanwhile, the diagnosis loss was set to be inversely proportional to the mask ratio, as a diagnosis can only be meaningful when there is ample unmasked information. This structure collectively ensured a balance between information concealment for learning and information availability for accurate diagnostics.

Assumed the mask ratio of images to be a random number  $0 \leq \alpha \leq 1$ . The corresponding mask ratio of reports would then be  $1 - \alpha$ . Then the diagnosis loss of the visual encoder was of weight  $1 - \alpha$ , and that of the linguistic encoder was of weight  $\alpha$ . We applied a binary cross-entropy loss to measure the forward diagnosis error ( $FDLoss$ ) between outputs and ground truth labels, as shown in Equation 1 where  $x$  represents the output probability and  $y$  represents the disease labels. Equations 2 and 3 illustrated the weights of visual  $DLoss$  ( $FVDLoss$ ) and linguistic  $DLoss$  ( $FLDLoss$ ) in the forward stage. In these formulas, The subscript  $n$  indexed the data point in a batch.  $y_n$  stood for the actual label or target of the  $n^{th}$  data point. In our scenario, 0 signified a negative outcome, 0.5 indicated an unclear or unspecified status, and 1 denoted a positive disease. The term  $x_n$  denoted the predicted probability that the  $n^{th}$  data point belongs to the positive class, a value predicted by the model that lies between 0 and 1.

$$FDLoss = y_n \cdot \log x_n + (1 - y_n) \cdot \log(1 - x_n) \quad (1)$$

$$FVDLoss = (1 - \alpha) \cdot (FDLoss) \quad (2)$$

$$FLDLoss = \alpha \cdot (FDLoss) \quad (3)$$

The image generation loss ( $IGLoss$ ) between the origin images and the generated images was estimated via MSE, while the report generation loss ( $RGLoss$ ) was calculated by CE. Equations 4 and 5 illustrate the calculation of weighted  $IGLoss$  and  $RGLoss$ . In these formulas,  $x$  denoted the input,  $y$  represented the target,  $w$  signifies the weight, and  $c$  indicated the number of classes (words).

$$IGLoss = \alpha \cdot (x_n - y_n)^2 \quad (4)$$

$$RGLoss = (1 - \alpha) \cdot - \sum_{c=1}^C w_c \log \frac{e^{x_{n,c}}}{\sum_{i=1}^C e^{x_{n,i}}} y_{n,c} \quad (5)$$

### Traceback Stage

The items generated by the decoders were traced back to the locked encoders. At this stage, the encoders are treated as a radiology expert trained in the forward stage, diagnosing based on the generated images and reports. Our primary focus was to evaluate the medical correctness of these generated masked items. Hence, the weights of the traceback visual ( $TVDLoss$ ) and linguistic loss ( $TLDLoss$ ) should correlate with their corresponding mask ratio, where  $TDLoss$  stands

for traceback diagnosis loss. To pass the self-assessment examined by the encoders, the decoders were encouraged to preserve medical information, and the multi-modal fusion module was encouraged to facilitate information exchange. However, this principle heavily dependent on the accuracy of the encoders, which led to significant fluctuations in the early stages of training. This problem was addressed by introducing a compensation mechanism: we reduced the weight of the traceback diagnosis loss if the encoders were not performing adequately, as shown in Equations 6, 7 and 8.

$$TDLoss = y_n \cdot \log x_n + (1 - y_n) \cdot \log(1 - x_n) \quad (6)$$

$$TVDLoss = (e^{-FVDLoss})(1 - \alpha) \cdot (TDLoss) \quad (7)$$

$$TLDLoss = (e^{-FVDLoss})\alpha \cdot (TDLoss) \quad (8)$$

This compensation mechanism allowed the model to prioritize improving the encoders’ diagnostic capabilities during the initial stages of the training process, with the weights of the traceback losses kept close to 0. As the encoders’ achieved higher accuracy over time, the weight assigned to the traceback loss was gradually increased. The model’s focus gradually shifted from pursuing morphological similarity to striving for semantic similarity.

## 4 Experimental Setup

### 4.1 Dataset

We conducted experiments on two well-benchmarked public datasets, Indiana University Chest X-ray (IU-Xray) [Demner-Fushman *et al.*, 2015] and MIMIC Chest X-ray (MIMIC-CXR) [Johnson *et al.*, 2019]. We split the data into training, validation, and testing subsets. For IU-Xray, we adopt the widely-accepted 7:1:2 data split as suggested in prior studies [Chen *et al.*, 2020; Chen *et al.*, 2021; Wang *et al.*, 2022a]. For MIMIC-CXR, we adhere to the official data split.

### 4.2 Evaluation Metrics

To measure the quality of generated medical report, we follow the standard practice [Wang *et al.*, 2022b; Chen *et al.*, 2020; Chen *et al.*, 2021; Wang *et al.*, 2022a] to adopt Bilingual Evaluation Understudy (BLEU) [Papineni *et al.*, 2002], Metric for Evaluation of Translation with Explicit Ordering (METEOR) [Lavie and Agarwal, 2007], Recall-Oriented Understudy for Gisting Evaluation - Longest Common Subsequence (ROUGE-L) [Lin, 2004], and Consensus-based Image Description Evaluation (CIDEr) [Vedantam *et al.*, 2015] as the evaluation metrics. These evaluation metrics are widely used in the field of NLP to assess the quality of generated reports [Chen *et al.*, 2020; Wang *et al.*, 2022a; Wang *et al.*, 2022b].

### 4.3 Experiment Settings

We compared the performance of DTrace against the state-of-the-art medical report generation methods: R2Gen [Chen *et al.*, 2020], R2GenCMN [Chen *et al.*, 2021], CMCL [Liu

*et al.*, 2021], AlignTransformer [You *et al.*, 2021], MC-Transformer [Wang *et al.*, 2022b] and XProNet [Wang *et al.*, 2022a]. For fair evaluation, the released code from the comparison methods was deployed in identical environments.

We also conducted an ablation study to measure the contribution of each component of our framework compared to the baseline model. The baseline is a uni-directional encoder-decoder framework incorporating ViT and the Transformer architectures. On the baseline, we first integrate an image generation and a multi-modal fusion module, so as to illustrate the improvements resulting from bi-directional learning, where the mask ratio (image-text) was switched between 0.75 0 and 0 0.85. Then, we demonstrate the advantages of dynamic learning compared to the fixed-ratio training strategy. Finally, we incorporate our traceback mechanism to assess its ability to capture semantic information.

## 4.4 Implementation Details

Our implementation of DTrace was realized using the PyTorch package [Paszke *et al.*, 2019]. Optimization of the gradient descent process was carried out utilizing the AdamW optimizer [Loshchilov and Hutter, 2017], with a set learning rate of  $10^{-4}$ . In the context of report generation, the beam search algorithm was employed, with a specified beam width of 3. The predefined maximum lengths for the reports were set at 60 and 100 for the IU-Xray and MIMIC-CXR datasets, respectively. Training of the model was performed on an NVIDIA RTX GeForce 3090 graphics card, with a designated mini-batch size of 16. To enhance the efficiency of training, the model initially underwent a pre-training phase, wherein it was conditioned to reconstruct images and reports based on the information inherent to their respective modalities, coupled with contrastive learning techniques. The selection of the optimal model was determined based on its performance on the validation set, evaluated through the average scores of BLEU, METEOR, ROUGE-L, and CIDEr metrics. Additional implementation details, including model parameters and training environment, were presented in the Supplementary Materials. Our code will be publicly available on GitHub upon publication.

## 5 Result and Discussion

### 5.1 Comparisons to Previous Methods

Table 1 presents comparison results against the state-of-the-art methods. Our DTrace demonstrates superior overall performance with its best performance in all metrics for IU-Xray and best in all but one metric (second-best in RG-L) for MIMIC-CXR. The improvement in the BLEU metric shows that our framework performs better in long-term accuracy. Compared to BLEU (precision-based) and Rouge-L (recall-based), METEOR and CIDEr focus on distinctive words and accommodate diverse image descriptions [Vedantam *et al.*, 2015]. DTrace also has a distinct advantage in being consistent between the two datasets with other methods having fluctuations. This is attributed to DTrace’s ability to incorporate information from different modalities at varying proportions during the training process.

Dataset	Model	BL-1	BL-2	BL-3	BL-4	MTR	RG-L	CDr
IU-Xray	R2Gen	0.470	0.304	0.211	0.157	0.197	0.364	0.342
	R2GenCMN	0.486	0.307	0.216	0.156	<u>0.212</u>	0.374	0.331
	CMCL*	0.473	0.305	0.217	0.162	0.186	0.378	-
	AlignTransformer*	0.484	0.313	0.225	0.173	0.204	<u>0.379</u>	-
	MCTransformer*	<u>0.496</u>	<u>0.319</u>	<u>0.241</u>	<u>0.175</u>	-	0.377	0.449
	XProNet	<u>0.466</u>	<u>0.297</u>	<u>0.206</u>	0.153	0.205	0.369	0.341
	DTrace (ours)	<b>0.516</b>	<b>0.353</b>	<b>0.278</b>	<b>0.204</b>	<b>0.233</b>	<b>0.386</b>	<b>0.469</b>
MIMIC-CXR	R2Gen	0.344	0.208	0.140	0.100	0.135	0.271	0.146
	R2GenCMN	0.327	0.211	0.148	0.109	0.137	<u>0.298</u>	0.135
	CMCL*	0.344	0.217	0.140	0.097	0.133	0.281	-
	AlignTransformer*	<u>0.378</u>	<u>0.235</u>	0.156	0.112	<u>0.158</u>	0.283	-
	MCTransformer*	0.351	0.223	<u>0.157</u>	<u>0.118</u>	-	0.287	<u>0.281</u>
	XProNet	0.332	0.219	0.154	0.115	0.138	<b>0.314</b>	0.152
	DTrace (ours)	<b>0.392</b>	<b>0.260</b>	<b>0.171</b>	<b>0.129</b>	<b>0.162</b>	<u>0.309</u>	<b>0.311</b>

Table 1: Performance comparison between our DTrace and existing report generation methods on the IU-Xray and MIMIC-CXR datasets. The best results are highlighted in bold and the second best are underlined. BL, MTR, RG-L and CDr are the abbreviations of evaluation metrics BLEU, METEOR, ROUGE-L and CIDEr. The symbol \* denotes that the results are cited from their original papers.

Model	BL-1	BL-2	BL-3	BL-4	MTR	RG-L	CDr
Encoder-Decoder (Baseline)	0.478	0.304	0.195	0.149	0.176	0.355	0.327
+ Bi-directional Generation	0.484	0.318	0.226	0.167	0.193	0.362	0.401
+ Dynamic Learning	0.493	0.324	0.239	0.172	0.209	0.377	0.409
+ Traceback Mechanism	0.516	0.353	0.278	0.204	0.233	0.386	0.469

Table 2: Ablation study on key components of our proposed DTrace on IU-Xray dataset. BL, MTR, RG-L and CDr are the abbreviations of evaluation metrics BLEU, METEOR, ROUGE-L and CIDEr

This outperformance suggests that our model, by capturing the pathology-critical information, is able to cater to scenarios where descriptions of the same radiology image differ in writing style and wording among radiologists. As an example, there is a ground truth sentence A, “the heart size is normal” and two generated sentences, B and C, “the heart size is enlarged” and “the heart size is within normal limit”. The cross-entropy between A and B is smaller than that between A and C. To minimize the cross-entropy loss, the generated text will tend to be a template that fits the majority of reports instead of prioritizing in correct semantic meaning. We mitigate this problem by introducing the traceback mechanism, where the generated reports are assessed by an encoder that has been trained to perform an accurate diagnosis. In this approach, the generated items’ semantic correctness is trained, and the weight of cross-entropy loss is diluted.

Our DTrace shows better performance than R2GenCMN, AlignTransformer, and XProNet, which we suggest is due to the advantages of dual-modal learning in facilitating cross-modal communication. It is further enhanced by the traceback mechanism. Because even without information from another modality, this modality itself has the ability to reconstruct its own form, and our traceback further forces the model to obtain semantic information from another modality. In the cross-modal fusion module, various modalities exchange and complement each other’s information, establishing a harmonious communication protocol between them,

which achieves the same effect as R2GenCMN and XProNet. Furthermore, this process is enhanced by the traceback mechanism, leading to improved performance.

## 5.2 Ablation Study

The results of our ablation study are presented in Table 2, demonstrating the contributions of each component.

### Bi-directional Dual-modal Generation

The inclusion of Bi-directional Generation nudged the scores from 0.478 to 0.484 on BL-1, 0.304 to 0.318 on BL-2, 0.195 to 0.226 on BL-3, and 0.149 to 0.167 on BL-4, indicating improvements in the model’s linguistic predictive and generative capabilities. MTR showed an increase from 0.176 to 0.193, suggesting a more refined translation quality or content matching. RG-L slightly increased from 0.355 to 0.362, indicating better preservation of the word order and content. The CDr significantly improved from 0.327 to 0.401, pointing to enhanced coherence and logical structuring in the generated content. This improvement substantiates the efficacy of Bi-directional Generation in bolstering the model’s capacity to understand the inner knowledge and context.

### Dynamic Learning

The implementation of Dynamic Learning saw a slight regression in BL-1 from 0.484 to 0.493, but comparatively larger improvements in BL-2 from 0.318 to 0.324, BL-3 from 0.226 to 0.239, and in BL-4 from 0.167 to 0.172. These



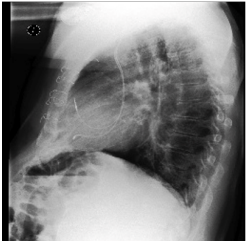
	Ground Truth	Encoder-Decoder	DTrace (Ours)
	The heart size remains normal. The mediastinal and hilar contours are unremarkable. Pulmonary vascularity is normal. The lungs are clear without focal consolidation. No pleural effusion or pneumothorax is present. There are mild degenerative changes in the thoracic spine.	The heart is of normal size with normal cardiomeastinal contours. The pulmonary vasculature is unremarkable. The lungs are clear without focal or diffuse abnormality. No radiopaque foreign body. Osseous structures are unremarkable. No radiopaque foreign bodies. No pleural effusion or pneumothorax is present. There are mild degenerative changes in the thoracic spine.	The lungs are well expanded and clear without focal consolidation pleural effusion or pneumothorax. Heart size is normal. Mediastinal silhouette and hilar contours are normal. There is no free air under the diaphragm. There are moderate degenerative changes in the thoracic spine.

Figure 4: An example of comparisons between traditional encoder-decoder architecture and our DTrace framework. The sentences are highlighted with different colors to represent the differences between the generated sequences and the ground truth report: (1) Green – sentences are consistent; (2) Blue – semantically similar sentences but different in expression; (3) Orange – missing sentences and, (4) Gray-italic – sentences not included in the ground truth.

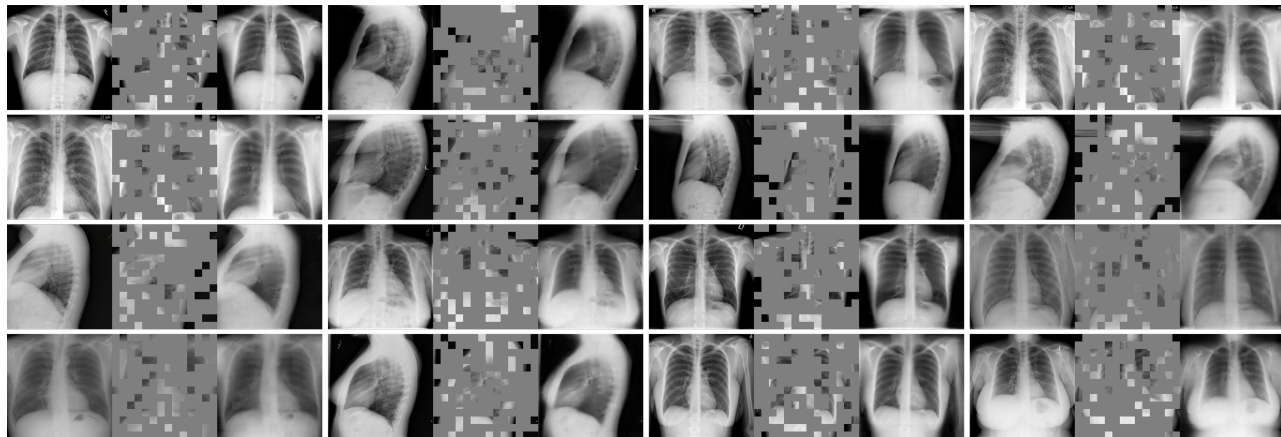


Figure 5: Visualization of reconstructed images with mask ratio 75% from the model. For each triplet, we show the origin image (left), the masked image (middle) and our reconstructed image (right)

metrics collectively indicate an improvement in the model’s ability to generate linguistically richer and more diverse content. MTR score experienced a substantial rise from 0.193 to 0.209. While RG-L witnessed an improvement, climbing back from 0.362 to 0.377, the CDr metric slightly improved from 0.401 to 0.409.

### Traceback Mechanism

Traceback Mechanism improved performance in all the metrics, with the largest in CIDEr from 0.401 to 0.469. This suggests that there are benefits in the training process for the model to identify and fill in missing semantic information across different modalities. This approach serves to: 1) foster communication between visual and linguistic, 2) constrain the medical validity of the generated report, 3) further mitigate the impact of varying writing styles on back-propagation, and 4) potentially align the information extracted from visual and linguistic sources to a consistent protocol.

### 5.3 Qualitative Analysis and Visualization

We conducted qualitative analyses of our DTrace framework against the baseline encoder-decoder framework. As an example in Figure 4, the baseline framework leaves out critical diagnosis statements, e.g., missing description of “mild degenerative changes in the thoracic spine”, while the DTrace-

generated report contains most of the diagnosis statements and shows high consistency with the ground-truth report. In addition, Figure 5 shows the images reconstructed from the 75%-masked images and unmasked report by our DTrace. The reconstructed images are highly consistent with the original unmasked images, demonstrating our DTrace’s potential for image reconstruction. Additional visualization examples are included in the supplementary materials.

## 6 Conclusion

In this study, we introduced a new medical report generation framework with dual-modal dynamic traceback learning (DTrace). In the DTrace, we introduced a traceback mechanism to supervise semantic correctness during the training process and a dynamic learning strategy to mitigate the reliance of existing generative cross-modal frameworks on textual information as the input. The experimental results demonstrate that the introduced traceback mechanism and dynamic learning strategy are effective in the dual-modal generation framework to improve medical report generation, which enabled our DTrace to achieve state-of-the-art performance in the well-benchmarked IU-Xray and MIMIC-CXR datasets.

## References

- [Cawsey *et al.*, 1997] Alison J Cawsey, Bonnie L Webber, and Ray B Jones. Natural language generation in health care. *Journal of the American Medical Informatics Association*, 4(6):473–482, 1997.
- [Chen *et al.*, 2020] Zhihong Chen, Yan Song, Tsung-Hui Chang, and Xiang Wan. Generating radiology reports via memory-driven transformer. In *Proceedings of the 2020 Conference on Empirical Methods in Natural Language Processing*, November 2020.
- [Chen *et al.*, 2021] Zhihong Chen, Yaling Shen, Yan Song, and Xiang Wan. Cross-modal memory networks for radiology report generation. In *Proceedings of the 59th Annual Meeting of the Association for Computational Linguistics and the 11th International Joint Conference on Natural Language Processing (Volume 1: Long Papers)*, pages 5904–5914, Online, August 2021. Association for Computational Linguistics.
- [Demner-Fushman *et al.*, 2015] Dina Demner-Fushman, Marc Kohli, Marc Rosenman, Sonya Shooshan, Laritza Rodriguez, Sameer Antani, George Thoma, and Clement McDonald. Preparing a collection of radiology examinations for distribution and retrieval. *Journal of the American Medical Informatics Association : JAMIA*, 23, 07 2015.
- [Devlin *et al.*, 2018] Jacob Devlin, Ming-Wei Chang, Kenton Lee, and Kristina Toutanova. Bert: Pre-training of deep bidirectional transformers for language understanding. *arXiv preprint arXiv:1810.04805*, 2018.
- [Dosovitskiy *et al.*, 2020] Alexey Dosovitskiy, Lucas Beyer, Alexander Kolesnikov, Dirk Weissenborn, Xiaohua Zhai, Thomas Unterthiner, Mostafa Dehghani, Matthias Minderer, Georg Heigold, Sylvain Gelly, et al. An image is worth 16x16 words: Transformers for image recognition at scale. *arXiv preprint arXiv:2010.11929*, 2020.
- [Geng *et al.*, 2022] Xinyang Geng, Hao Liu, Lisa Lee, Dale Schuurmans, Sergey Levine, and Pieter Abbeel. Multimodal masked autoencoders learn transferable representations. *arXiv preprint arXiv:2205.14204*, 2022.
- [He *et al.*, 2022] Kaiming He, Xinlei Chen, Saining Xie, Yanghao Li, Piotr Dollár, and Ross Girshick. Masked autoencoders are scalable vision learners. In *Proceedings of the IEEE/CVF conference on computer vision and pattern recognition*, pages 16000–16009, 2022.
- [Irvin *et al.*, 2019] Jeremy Irvin, Pranav Rajpurkar, Michael Ko, Yifan Yu, Silvana Ciurea-Ilcus, Chris Chute, Henrik Marklund, Behzad Haghgoo, Robyn Ball, Katie Shpankaya, et al. Chexpert: A large chest radiograph dataset with uncertainty labels and expert comparison. In *Proceedings of the AAAI conference on artificial intelligence*, volume 33, pages 590–597, 2019.
- [Johnson *et al.*, 2019] Alistair Johnson, Tom Pollard, Seth Berkowitz, Nathaniel Greenbaum, Matthew Lungren, Chih-ying Deng, Roger Mark, and Steven Horng. Mimic-cxr, a de-identified publicly available database of chest radiographs with free-text reports. *Scientific Data*, 6:317, 12 2019.
- [Lavie and Agarwal, 2007] Alon Lavie and Abhaya Agarwal. Meteor: An automatic metric for mt evaluation with high levels of correlation with human judgments. In *Proceedings of the Second Workshop on Statistical Machine Translation*, StatMT '07, page 228–231, USA, 2007. Association for Computational Linguistics.
- [Lin, 2004] Chin-Yew Lin. ROUGE: A package for automatic evaluation of summaries. In *Text Summarization Branches Out*, pages 74–81, Barcelona, Spain, July 2004. Association for Computational Linguistics.
- [Liu *et al.*, 2021] Fenglin Liu, Shen Ge, and Xian Wu. Competence-based multimodal curriculum learning for medical report generation. In *Proceedings of the 59th Annual Meeting of the Association for Computational Linguistics and the 11th International Joint Conference on Natural Language Processing (Volume 1: Long Papers)*, pages 3001–3012, Online, August 2021. Association for Computational Linguistics.
- [Liu *et al.*, 2023] Gang Liu, Pengfei Li, Zixu Zhao, Jinlong He, Genrong He, and Shenjun Zhong. Cross-modal self-supervised vision language pre-training with multiple objectives for medical visual question answering. 2023.
- [Loshchilov and Hutter, 2017] Ilya Loshchilov and Frank Hutter. Decoupled weight decay regularization. *arXiv preprint arXiv:1711.05101*, 2017.
- [Lu *et al.*, 2022] Haoyu Lu, Qiongyi Zhou, Nanyi Fei, Zhiwu Lu, Mingyu Ding, Jingyuan Wen, Changde Du, Xin Zhao, Hao Sun, Huiguang He, et al. Multimodal foundation models are better simulators of the human brain. *arXiv preprint arXiv:2208.08263*, 2022.
- [Messina *et al.*, 2022] Pablo Messina, Pablo Pino, Denis Parra, Alvaro Soto, Cecilia Besa, Sergio Uribe, Marcelo Andía, Cristian Tejos, Claudia Prieto, and Daniel Capurro. A survey on deep learning and explainability for automatic report generation from medical images. *ACM Computing Surveys (CSUR)*, 54(10s):1–40, 2022.
- [Moon *et al.*, 2022] Jong Hak Moon, Hyungyung Lee, Woncheol Shin, Young-Hak Kim, and Edward Choi. Multimodal understanding and generation for medical images and text via vision-language pre-training. *IEEE Journal of Biomedical and Health Informatics*, 26(12):6070–6080, 2022.
- [Papineni *et al.*, 2002] Kishore Papineni, Salim Roukos, Todd Ward, and Wei-Jing Zhu. Bleu: A method for automatic evaluation of machine translation. In *Proceedings of the 40th Annual Meeting on Association for Computational Linguistics*, ACL '02, page 311–318, USA, 2002. Association for Computational Linguistics.
- [Paszke *et al.*, 2019] Adam Paszke, Sam Gross, Francisco Massa, Adam Lerer, James Bradbury, Gregory Chanan, Trevor Killeen, Zeming Lin, Natalia Gimelshein, Luca Antiga, et al. Pytorch: An imperative style, high-performance deep learning library. *Advances in neural information processing systems*, 32, 2019.



- [Stefanini *et al.*, 2021] Matteo Stefanini, Marcella Cornia, Lorenzo Baraldi, Silvia Cascianelli, Giuseppe Fiameni, and Rita Cucchiara. From show to tell: A survey on image captioning. *arXiv preprint arXiv:2107.06912*, 2021.
- [Taud and Mas, 2018] Hind Taud and JF Mas. Multilayer perceptron (mlp). *Geomatic approaches for modeling land change scenarios*, pages 451–455, 2018.
- [Vaswani *et al.*, 2017] Ashish Vaswani, Noam Shazeer, Niki Parmar, Jakob Uszkoreit, Llion Jones, Aidan N Gomez, Łukasz Kaiser, and Illia Polosukhin. Attention is all you need. *Advances in neural information processing systems*, 30, 2017.
- [Vedantam *et al.*, 2015] Ramakrishna Vedantam, C Lawrence Zitnick, and Devi Parikh. Cider: Consensus-based image description evaluation. In *Proceedings of the IEEE conference on computer vision and pattern recognition*, pages 4566–4575, 2015.
- [Vinyals *et al.*, 2015] Oriol Vinyals, Alexander Toshev, Samy Bengio, and Dumitru Erhan. Show and tell: A neural image caption generator. In *Proceedings of the IEEE conference on computer vision and pattern recognition*, pages 3156–3164, 2015.
- [Wang *et al.*, 2022a] Jun Wang, Abhir Bhalerao, and Yulan He. Cross-modal prototype driven network for radiology report generation. In *European Conference on Computer Vision*, pages 563–579. Springer, 2022.
- [Wang *et al.*, 2022b] Zhanyu Wang, Hongwei Han, Lei Wang, Xiu Li, and Luping Zhou. Automated radiographic report generation purely on transformer: A multicriteria supervised approach. *IEEE Transactions on Medical Imaging*, 41(10):2803–2813, 2022.
- [Xiao *et al.*, 2023] Junfei Xiao, Yutong Bai, Alan Yuille, and Zongwei Zhou. Delving into masked autoencoders for multi-label thorax disease classification. In *Proceedings of the IEEE/CVF Winter Conference on Applications of Computer Vision*, pages 3588–3600, 2023.
- [You *et al.*, 2021] Di You, Fenglin Liu, Shen Ge, Xiaoxia Xie, Jing Zhang, and Xian Wu. Aligntransformer: Hierarchical alignment of visual regions and disease tags for medical report generation. In *Medical Image Computing and Computer Assisted Intervention—MICCAI 2021: 24th International Conference, Strasbourg, France, September 27–October 1, 2021, Proceedings, Part III 24*, pages 72–82. Springer, 2021.